Star Formation in Galaxies
"Recent" Developments

- Evolution Synthesis Models as previously discussed in the stars lecture (Tinsley 1968)
- The study of Blue Galaxies showed that starbursts were important in low-mass & interacting galaxies (Larson & Tinsley 1978)
- Near-UV & infrared star formation rate (SFR) diagnostics (1976 – 1986)
- IRAS detections of a significant population of infrared (IR) starburst galaxies (mid-1980s)
- Lyman-Break z=3 Galaxies (Steidel 1996) / HDF
- SCUBA detections of a population of high-z IR starburst galaxies (Smail 1997; Hughes 1998; Barger 1998)

General Features in Galaxy Spectra

- Methods by which SFR are calculated requires some knowledge of the spectral feature of galaxies
- The following slides are a summary of spectral features…

Rise in Blue Continuum from E to Sm/Irr

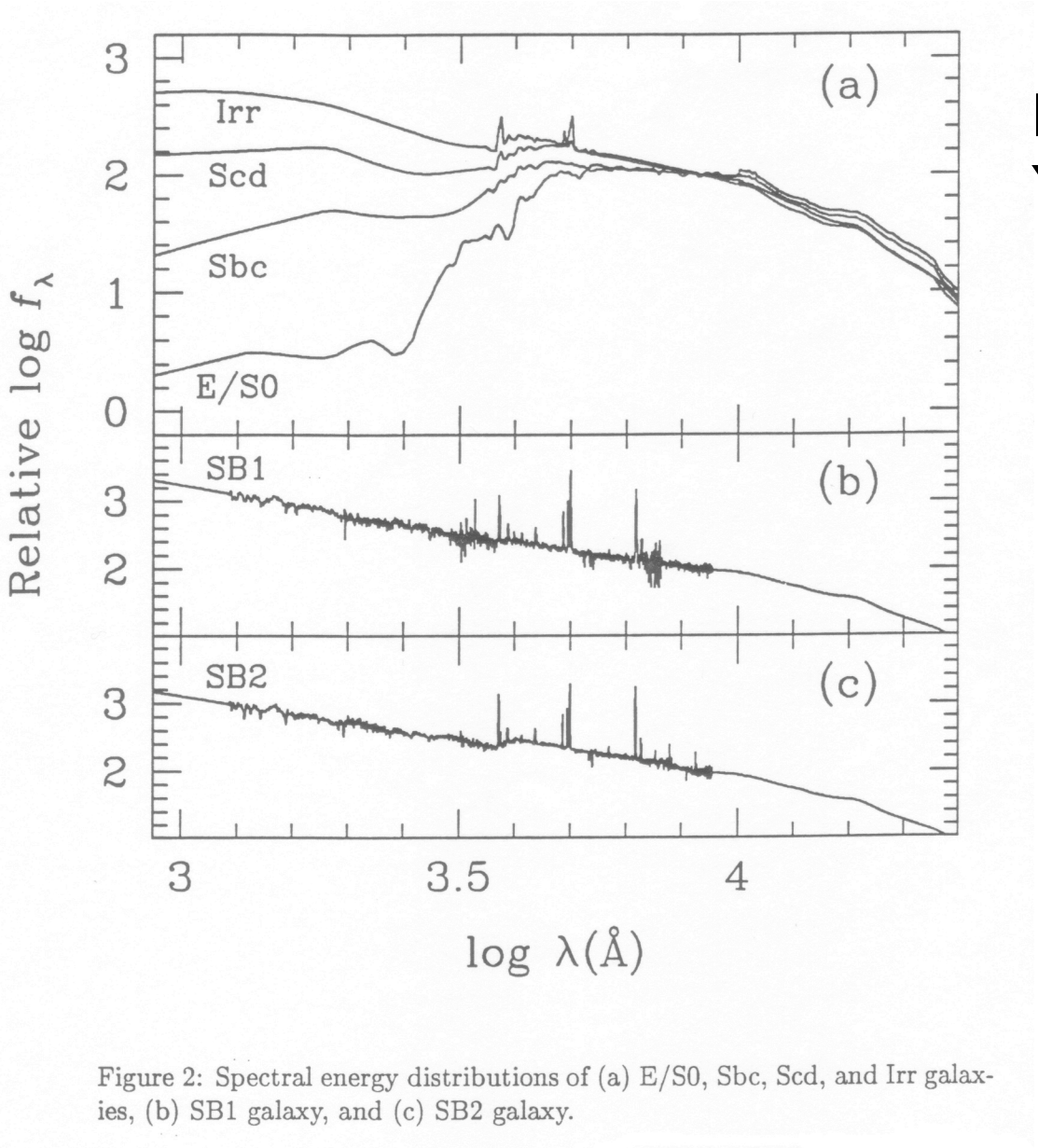

Figure 2: Spectral energy distributions of (a) E/S0, Sbc, Scd, and Irr galaxies, (b) SB1 galaxy, and (c) SB2 galaxy.

Due to an increase in Young Blue Stars

(Yahata et al. 2000)

Composite Spectrum: E to S

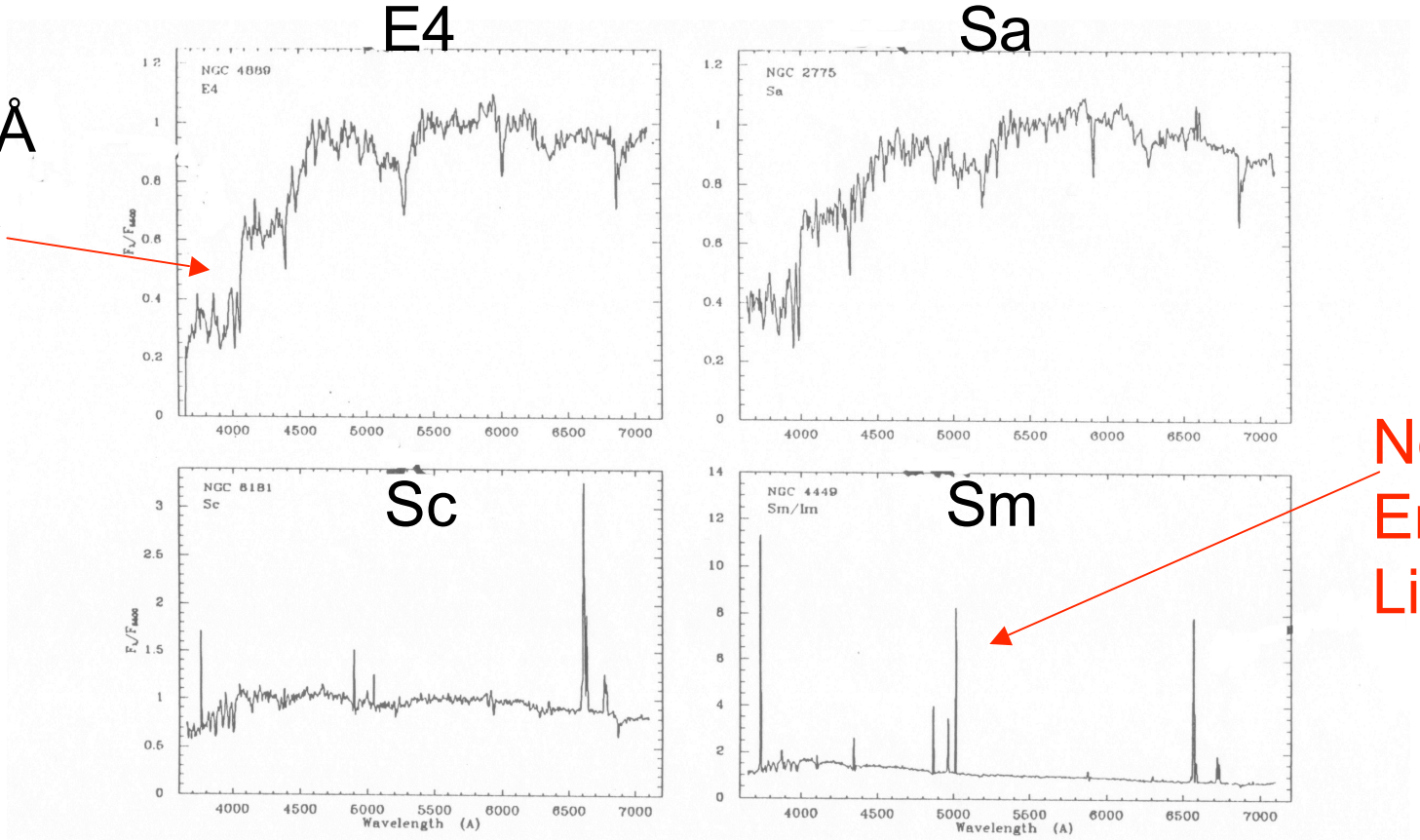

4000 Å Break

Nebular Emission Lines

(Kennicutt 1998)

Figure 1: *Integrated spectra of elliptical, spiral, and irregular galaxies, from Kennicutt (1992b). The fluxes have been normalized to unity at 5500 Å.*

- Change: K-Giants (3 – 15 Gyr old) → A-stars (1 < Gyr old)
- Increase in Nebulae Emission Lines

Nebulae Emission Lines

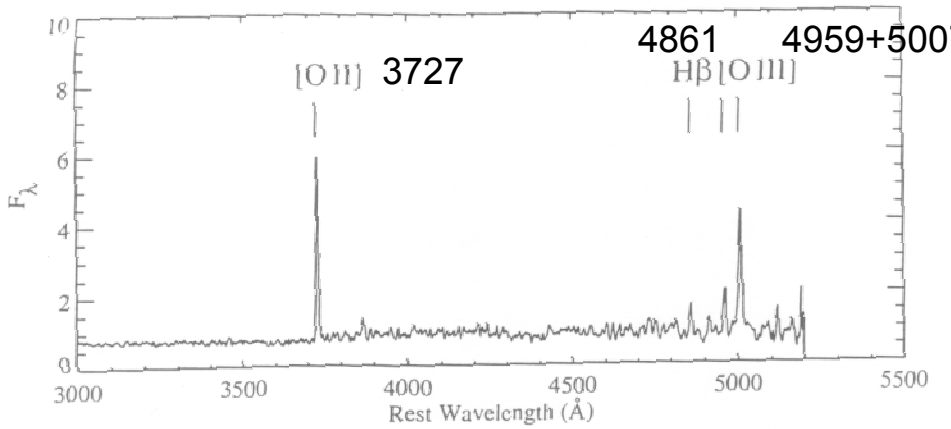

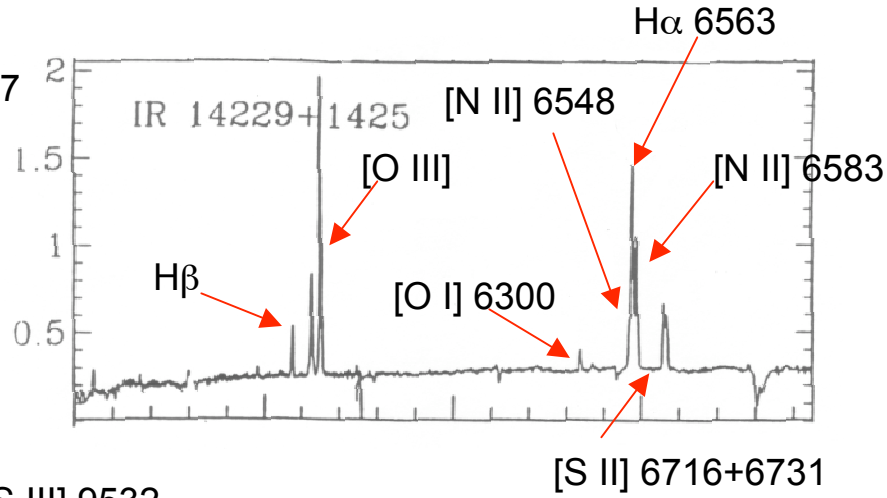

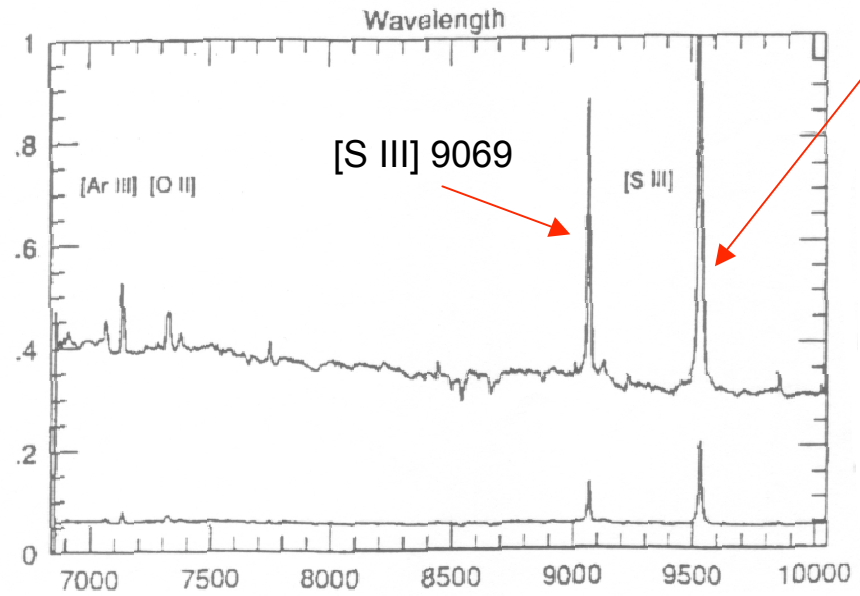

Ionization by
1) OB Stars
2) Supernovae
3) AGN

Note: [O III] = O^{++}, etc.

(Cowie et al. 1995; Kim et al. 1995; Osterbrock et al. 1992)

4000 Angstrom Break

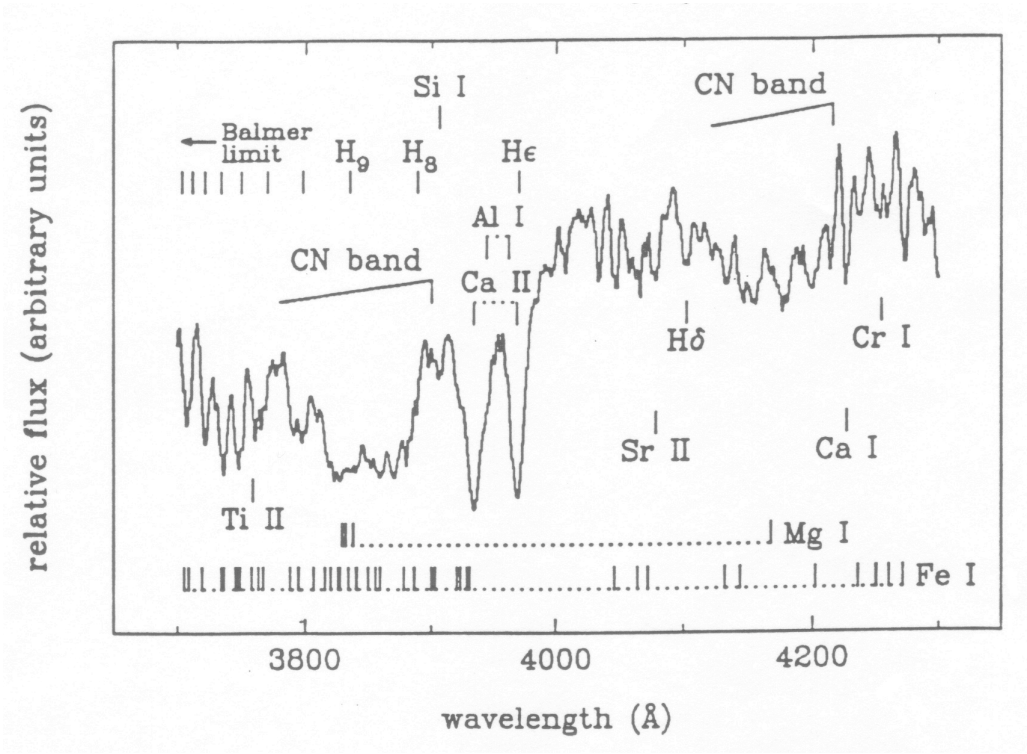

Fig. 1. Spectrum of the star HD72324 (G9 III) in the region around the λ4000 Å break. As a reference, we have also plotted the most intense (EW > 200 mÅ) Fraunhofer lines from the sun (using the tabulated data from Lang 1974 —original source Moore et al. 1966—), together with the Balmer lines and two CN molecular bands (the central bandpass of the CN3883 index defined by Pickles 1985, and the absorption band of the S(4142) index employed by Smith et al. 1997) which can be found in this spectral range. The contribution of the atomic metallic lines, especially from Fe I and Mg I, becomes very important bluewards λ4000 Å.

- Caused by the Calcium II Absorption Doublet
- And line blanketing of Metal Lines

(Gorgas, Cadiel, Pedraz, & Gonzalez 1999)

Lyman Break Galaxies:

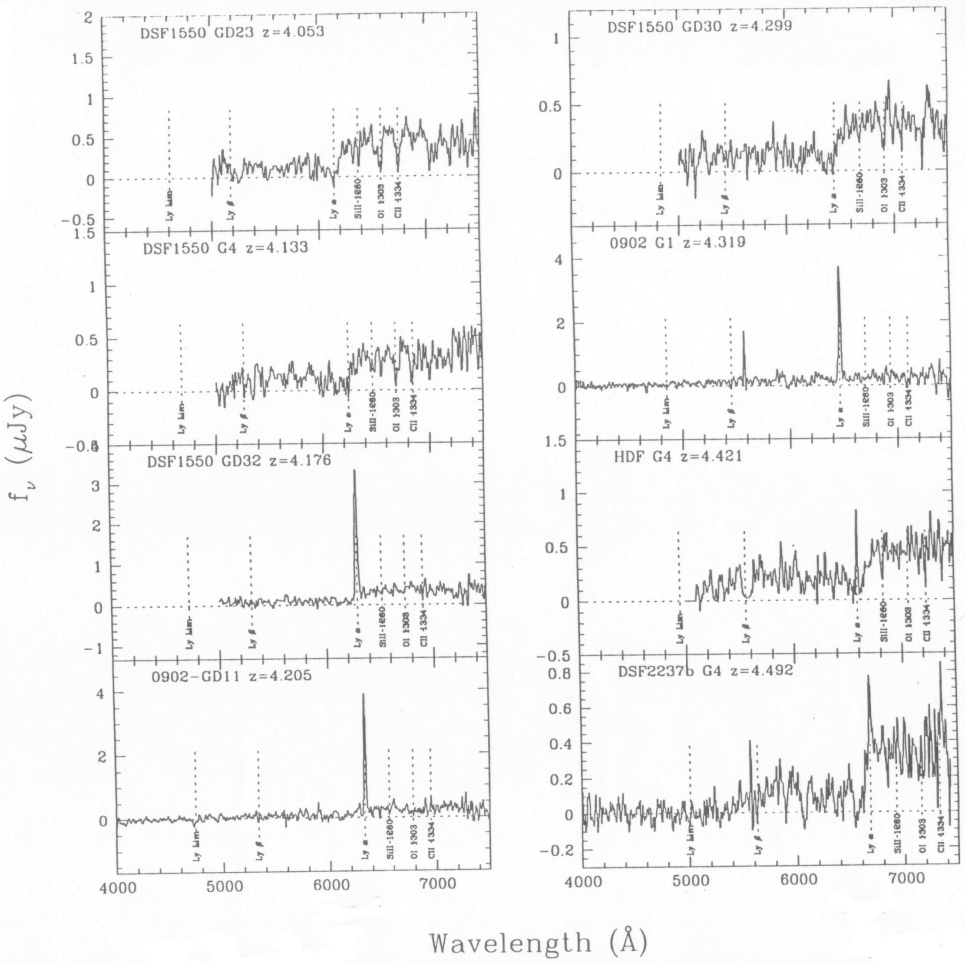

FIG. 3.—Example spectra of *G*-band break objects. Note that, as for the $z \sim 3$ sample, the $z \sim 4$ Lyman-break galaxies have a widely varying Lyα line strength, from strong emission lines, to very strong and broad absorption. Overall, the spectra are very similar to the $z \sim 3$ objects at correspondingly bright UV luminosities.

(Steidel et al. 1999)

- UV Photons with $\lambda_{rest} < 912$ Å ionize H atoms
- UV Photons with $\lambda_{rest} <$ Lyα are absorbed by line-of-sight H clouds as λ is redshifted

Synthesis Models

- Construct stellar evolutionary tracks containing parameters such as T_{eff}, L_{bol}, & $L_{H\alpha}$. These are typically obtained via atmospheric models & spectral libraries
- Construct IMFs containing parameters such as Luminosity, Color, Spectra of Single Age Population
- Add together IMFs from step 2 to get spectra & colors of a galaxy with an arbitrary star formation history

Synthesis Models, cont.

- The Free Parameters are:

    1) Star Formation History
    2) Galaxy Age
    3) Metal Abundance
    4) IMF

- General Uncertainties are:

    1) Dust Extinction
    2) IMF
    3) Galaxy Age
    4) Metallicity
    5) Star Formation History

Diagnostic Methods

- UV Continuum
- Recombination Lines
- Forbidden Lines
- Far Infrared
- Radio
- X-ray

Certain SFR Diagnostics are chosen over others due to

1) Limited availability of λ coverage for galaxy in question
2) Bias of observer

1) UV Continuum

- Continuum emission in λ = 1250 – 2500 Å comes primarily from young, massive stars
- Thus, L_{UV} is a measure of present SFR,

$$\mathrm{SFR} \propto L_{(1250-2500\mathrm{\AA})}.$$

- The calibration commonly used is,

$$\mathrm{SFR}(\mathrm{M}_\odot\ \mathrm{yr}^{-1}) = 1.4 \times 10^{-28} L_\nu\ (\mathrm{ergs\ s^{-1}\ Hz^{-1}}).$$

Note that L_ν is flat over λ = 1250 – 2500 Å

SFR_{UV}, cont.

- Assumptions:
  1) Δt » 10^8 yr (note that $\tau_{UV\ stars} < 10^8$ yr).
  2) Salpeter IMF (i.e., $\xi(M) \sim M^{-2.35}$).
  3) Stellar mass range of 0.1 – 100 M_{sun}
- Advantages:
  1) L_{UV} is from the photospheres of young stars
  2) This technique is applicable to galaxies over z = 1 – 5.
- Disadvantages:
  1) This method is sensitive to extinction
  2) Sensitive to IMF assumed. I.e., L_{UV} traces > 5 M_{sun} stars, so extrapolations to low-mass stars are uncertain

2) Recombination Lines

- Recombination lines are the re-emission of integrated stellar luminosity of photons blueward of 912 Å (i.e., ionizing photons).
- It is thus a direct probe of young, massive stars
- Contributors: Stars with masses > 10 M_{sun}, and thus $\Delta t <$ 20 Myr
- I.e., Instantaneous star formation
- Two common calibrations:

$$\mathrm{SFR}(\mathrm{M}_\odot\ \mathrm{yr}^{-1}) = 7.9 \times 10^{-42} L_{\mathrm{H}\alpha}\ (\mathrm{ergs\ s}^{-1}),$$

$$\mathrm{SFR}(\mathrm{M}_\odot\ \mathrm{yr}^{-1}) = 8.2 \times 10^{-40} L_{\mathrm{Br}\gamma}\ (\mathrm{ergs\ s}^{-1}).$$

SFR via Recombination Lines, cont.

- Assumptions:

  1) A Salpeter IMF
  2) Stars of Masses 0.1 – 100 M_{sun}
  3) Case B (low density) recombination at T_e = 10,000 K

- Advantages:

  1) Recombination Lines are strong & thus detectable
  2) Direct coupling between nebular emission & massive SF
  3) Hα can be detected out to z » 2

- Disadvantages:

  1) Recombination lines are subject to Extinction
  2) Sensitivity to IMF used (i.e., $SFR_{Scalo} \neq SFR_{Salpeter}$)

3) Forbidden Lines

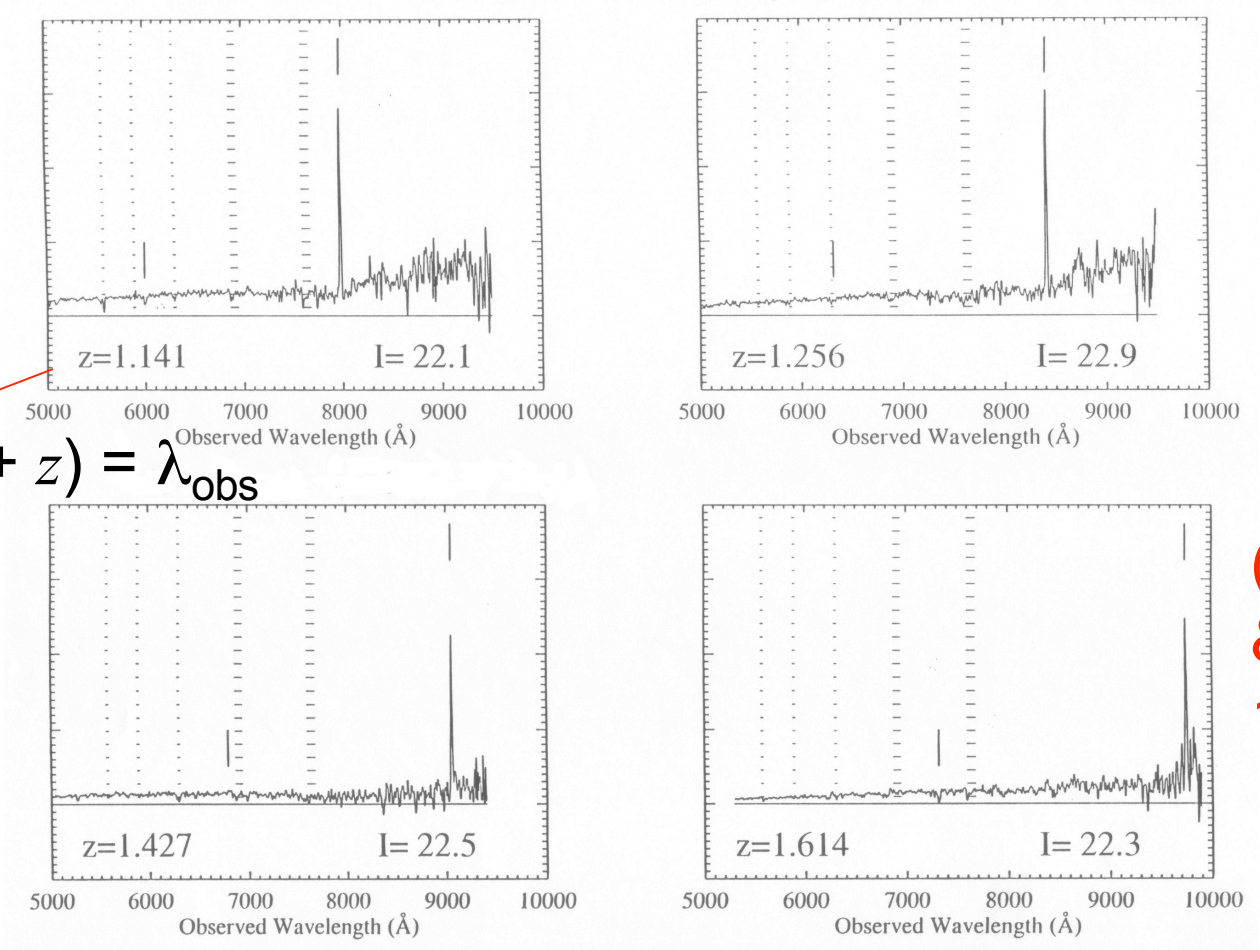

$\lambda_{rest}\,(1 + z) = \lambda_{obs}$

(Cowie, Hu, & Songaila 1995)

- In the redshift range 0.5 – 1.6, Hα is redshifted out of the optical range. Thus, it is sometimes more useful to calibrate SFR based on the [O II] λ3727 line

SFR Forbidden Lines, cont.

- The excitation of [O II] λ3727 is not coupled with the ionizing luminosity of young stars, but we can use the average of its flux density with that of Hα to determine a SFR.
- Commonly used calibration:

$$\mathrm{SFR}(\mathrm{M}_\odot\ \mathrm{yr}^{-1}) = (1.4 \pm 0.4) \times 10^{-41} L_{[\mathrm{OII}]}\ (\mathrm{ergs\ s}^{-1}),$$

where the error represents the range in the [O II] / Hα ratio from blue emission-line galaxies (the low end) to luminous spirals & IR galaxies (the high end)

SFR Forbidden Lines

- Advantages:

    1) [O II] is readily visible to z ~ 1.6

- Disadvantages:

    1) [O II] / Hα varies wildly from galaxy to galaxy
    2) [O II] is subject to extinction
    3) The luminosity of [O II] is sensitive to abundances & ionization state of the gas. We will discuss this later.

4) Far Infrared

- A significant fraction of L_{bol} in luminous starburst galaxies is absorbed by dust & re-emitted in the thermal IR (10 – 300 μm).
- The absorption cross section for dust peaks in the UV, thus the IR traces light from young, massive stars.
- Commonly used calibration:

$$\mathrm{SFR}(\mathrm{M}_\odot\ \mathrm{yr}^{-1}) = 4.5 \times 10^{-44} L_{\mathrm{IR}}\ (\mathrm{ergs\ s}^{-1}).$$

SFR_{IR}, cont.

- Assumptions:
  1) An optical depth $\tau \gg 1$ (i.e., $L_{IR} \sim L_{SB}$)
  2) Continuous burst $\Delta t \sim 10 - 100$ Myr
  3) Salpeter IMF
- Ideal for SF starburst galaxies because:
  1) Young stars dominate UV-optical radiation
  2) $\tau > 1$
  3) $L_{IR} \sim L_{SB}$
- Not ideal for SF in disks of normal galaxies because:
  1) While λ (~ 60 μm) $\rightarrow$ "warm" component heated by young stars
  2) λ (> 100 μm) $\rightarrow$ "IR cirrus" heated by interstellar radiation field (i.e., the old stellar population)

5) Radio Emission from Galaxies

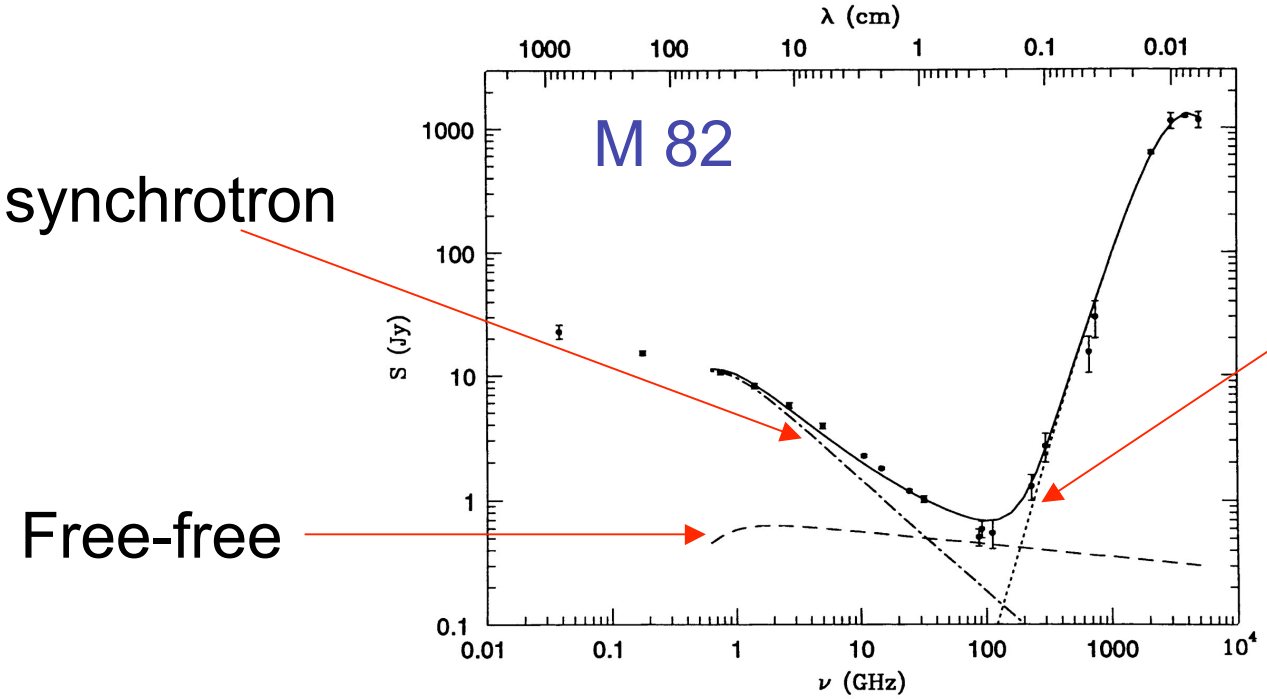

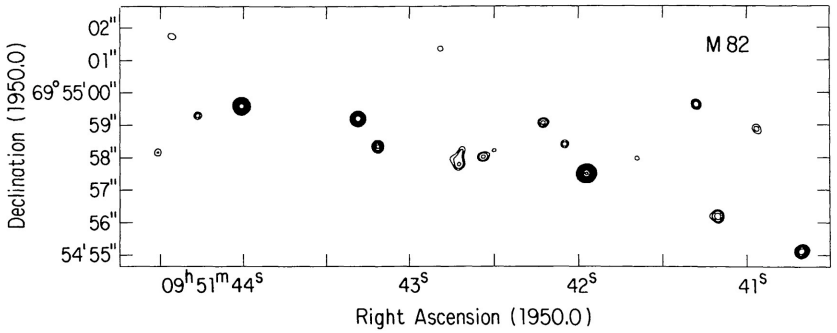

Figure 7 The compact sources visible in this 8.44 GHz VLA map (Z.-P. Huang, unpublished data) of the center of M82 are radio SNRs, the faintest of which are about as luminous as the Galactic SNR Cassiopeia A. The logarithmic contours are separated by factors of $2^{1/2}$ in brightness, and the lowest contour is 0.5 mJy beam^{-1}.

Supernova remnants (SNRs) in M82

(Condon 1992, ARAA)

Far-infrared - Radio Correlation

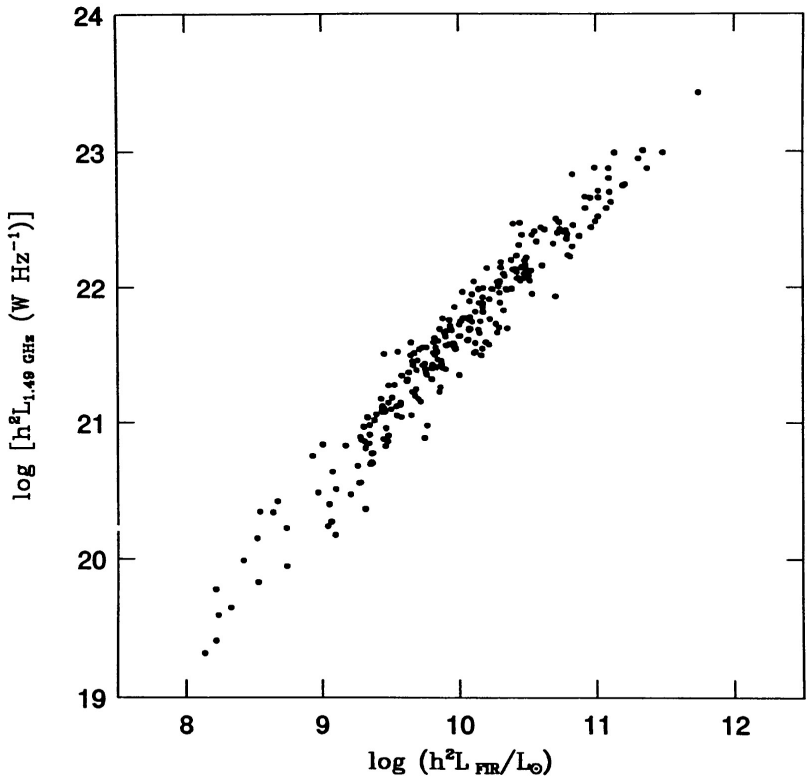

Figure 8 The FIR/radio correlation for strong sources selected at $\lambda = 60$ μm and not containing known monsters (e.g. Seyfert nuclei) or optically thick to free-free absorption at $\nu = 1.49$ GHz. The measurement errors are smaller than the intrinsic scatter for this sample. Abscissa: log FIR luminosity in solar units. Ordinate: log 1.49 GHz luminosity (W Hz^{-1}).

- There is a correlation between FIR and radio luminosity for spiral & starburst galaxies that has led to the radio being used as a SFR tracer.
- A common parameter used is *q*, where,

$$q = log\left(\frac{FIR}{3.75 \times 10^{12}\mathrm{W\ m^{-2}}}\right) - log\left(\frac{S_{1.4\mathrm{GHz}}}{\mathrm{W\ m^{-2}\ Hz^{-1}}}\right)$$

- Note that <*q*> ~ 2.3 for spiral & starburst galaxies.

Radio Emission

- Radio Emission is synchrotron emission associated with SNRs of 8 M_{sun} stars (t_{life} < 3x10^7 yr), but also can be generated by AGN.
- Note that t_{life}(relativistic e-) < 10^8 yr. I.e., recent SF.
- A calibration for 1.4 GHz emission:

$$SFR = 1.4 \times 10^{-28} \left(\frac{L_{1.4\mathrm{GHz}}}{\mathrm{ergs\ \ s^{-1}\ \ Hz^{-1}}} \right) \quad M_\odot \ \ yr^{-1}$$

- See Condon (1992, ARAA), Haarsma et al. (2000), and Sullivan et al. (2001) for more details

Radio Emission

- Advantages:
    1) Radio emission is not overwhelmed by emission from stellar populations older than 10^8 yr.
    2) Radio maps can be made with subarcsecond positional accuracy & resolution
    3) Radio emission is transparent in dusty environments
- Disadvantages:
    1) Free-free emission can be an important component of radio emission from a galaxy at 1 - 2 GHz.
    2) AGN also are strong synchrotron sources

6) X-rays

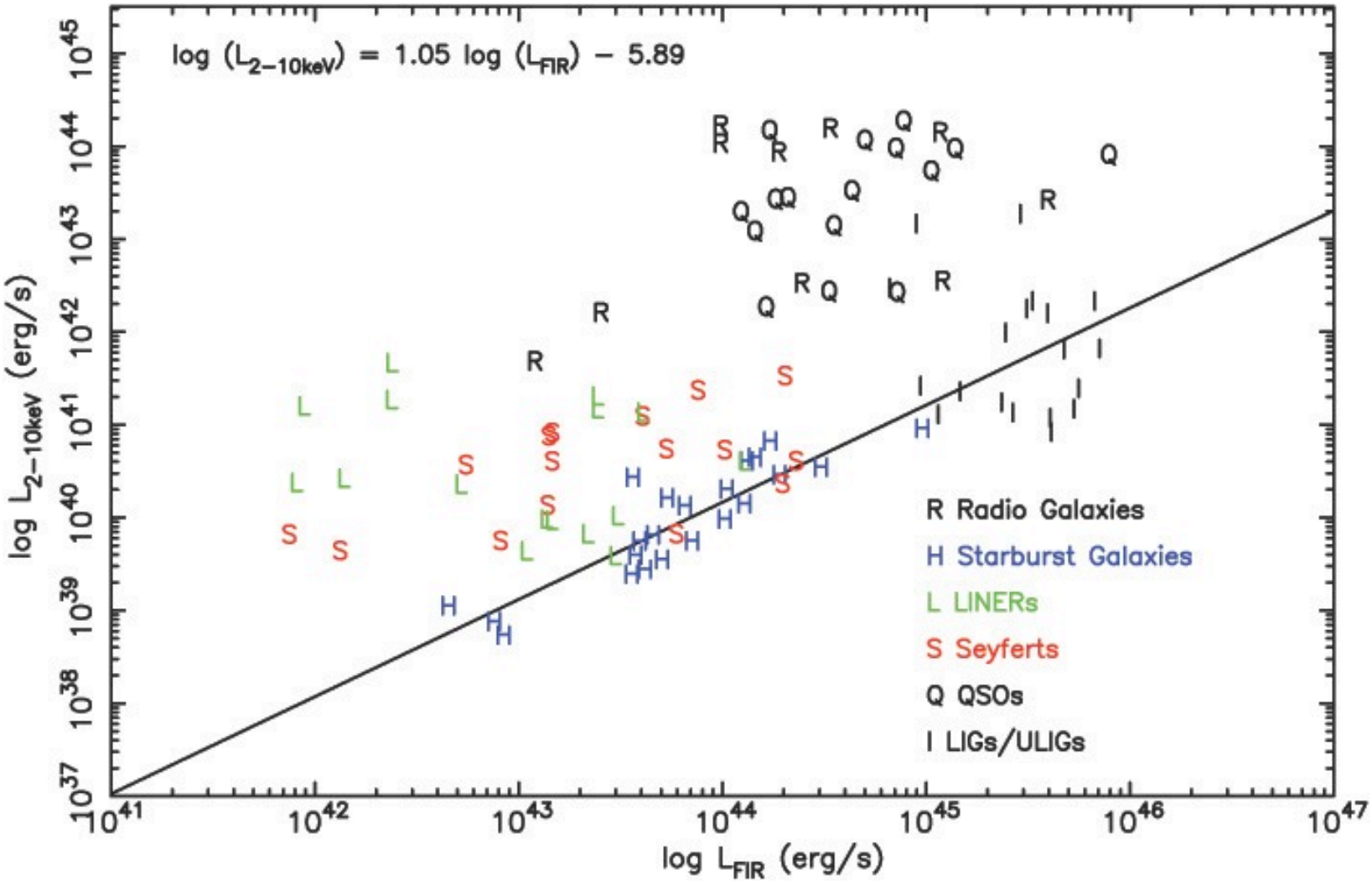

(e.g., Trentham et al. 2004)

X-rays as Star Formation rate indicator

- $L_X \sim L_{IR} \sim$ SFR
- L_X is from high mass X-ray binaries (neutron star/black hole accretion from a normal > 10 M_{sun} mass companion star; characteristic timescale ~ nuclear timescale ~ 2×10^7 yr)
- Assumptions are the same as for SFR via IR diagnostic

(Grimm et al. 2003; Ranalli et al. 2003)

Star Formation Along the Hubble Sequence

- Disks of Galaxies

  - UV and Ha are good tracers

- Nuclei of Galaxies

  - SF triggered by mergers/interactions & bars
  - gas dissipates & flows to the center of the galaxy
  - IR is the best tracer

Equivalent Width

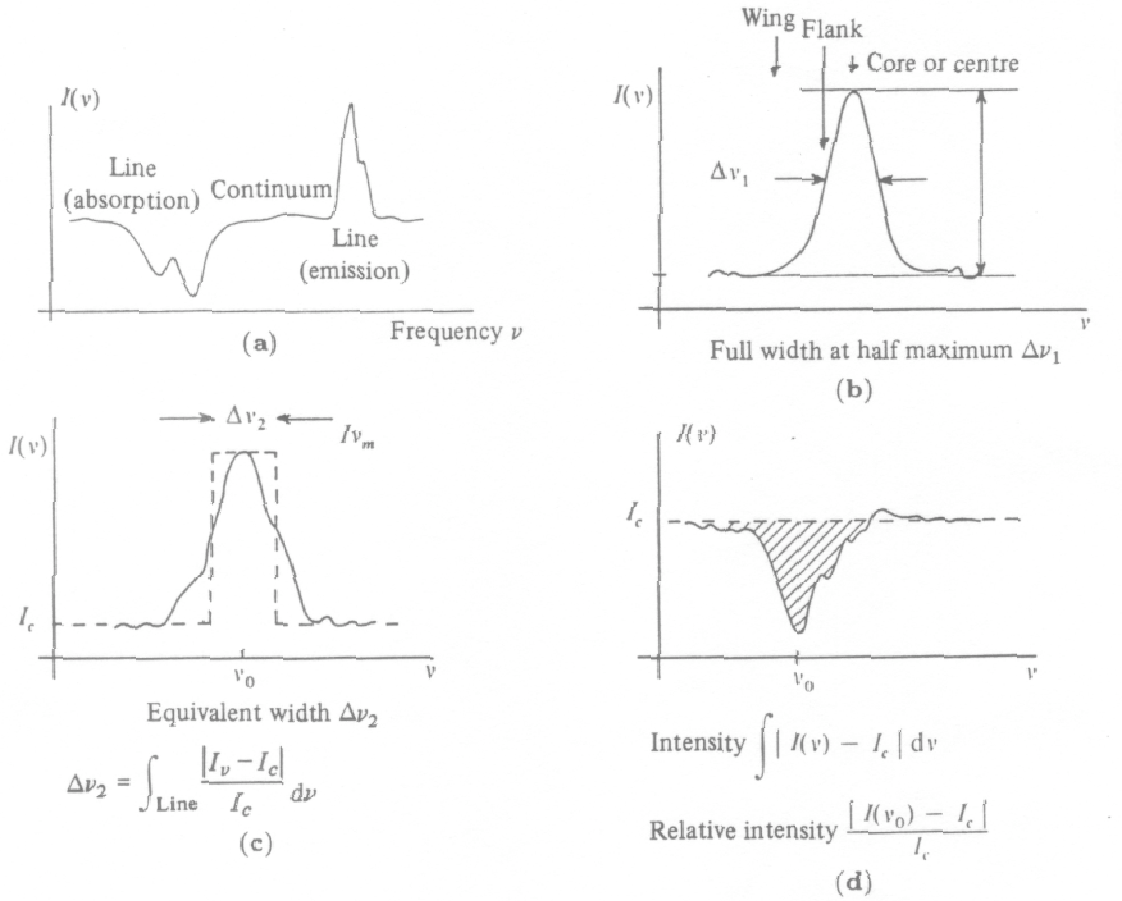

Fig. 7.1a–d. Terminology for spectral lines. (a) Arbitrary spectrum. (b) Full width at half-maximum of an emission line. (c) Equivalent width of a line. Definition applies for absorption or emission lines. (d) Relative intensity of an absorption line

$$\Delta\nu_2 = \int_{\text{Line}} \frac{|I_\nu - I_c|}{I_c} d\nu,$$

I_ν = intensity at ν

I_c = continuum intensity

W_λ (Hα) = SFR / L_{red}

How Does SFR Change with H.T.?

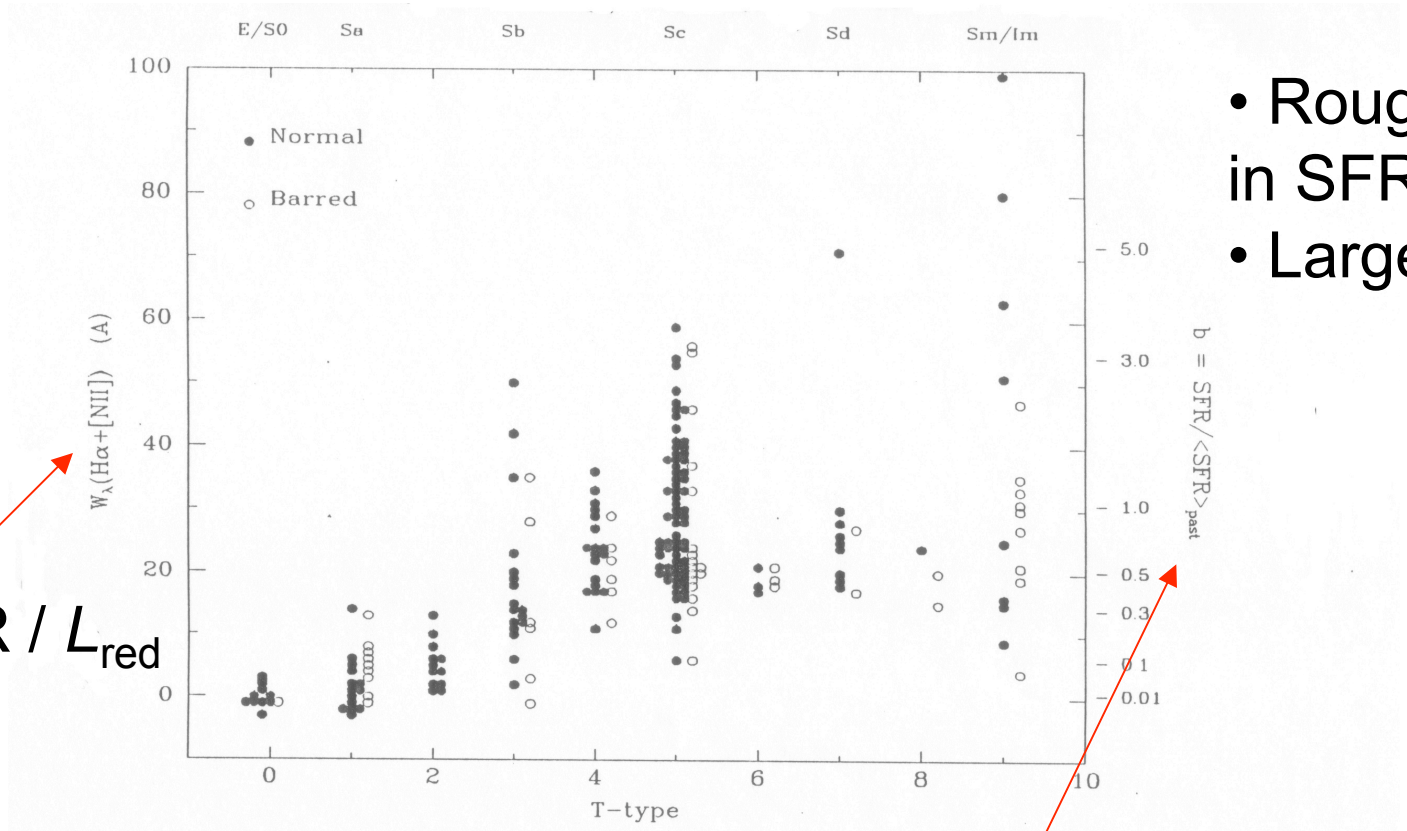

Figure 3: *Distribution of integrated Hα+[NII] emission-line equivalent widths for a large sample of nearby spiral galaxies, subdivided by Hubble type and bar morphology. The right axis scale shows corresponding values of the stellar birthrate parameter b, which is the ratio of the present SFR to that averaged over the past, as described in Section 5.1.*

- Rough increase in SFR with H. T.
- Large Scatter

SFR / L_{red}

$$b = \frac{\text{SFR}}{<\text{SFR}>_{\text{past}}} = \frac{\text{present SF}}{\text{average SF}}$$

Increase in SFR with HT, cont.

Hα observations of HII regions & the continuum luminosity Function estimates of OB associations have shown that the Increase in SFR is due to:

1) increase in the # of SF regions per unit mass/area
2) increase in masses of individual regions

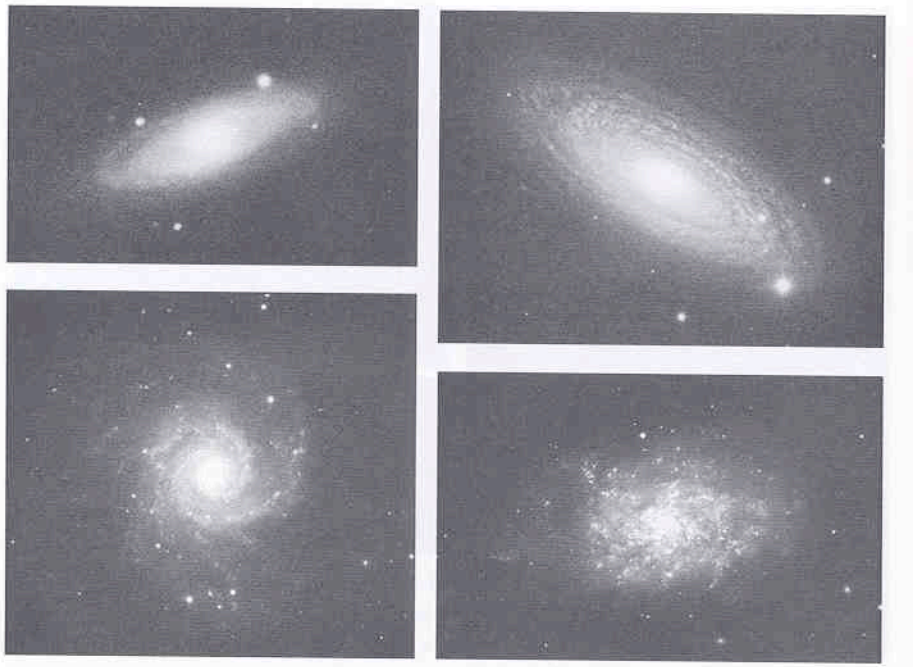

Figure 4.6 Four normal spiral galaxies: at top left NGC 2811 (Sa); at top right NGC 2841 (Sb); at lower left NGC 628 (Sc); at lower right NGC 7793 (Sd). [Photographs from the *Carnegie Atlas* courtesy of A. Sandage]

The range in SFR values per HT is due to

- Variations in gas content
- Nuclear Emission
- Interactions
- Short-term variability in SFR in individual galaxies

L_{IR} / L_H vs. HT

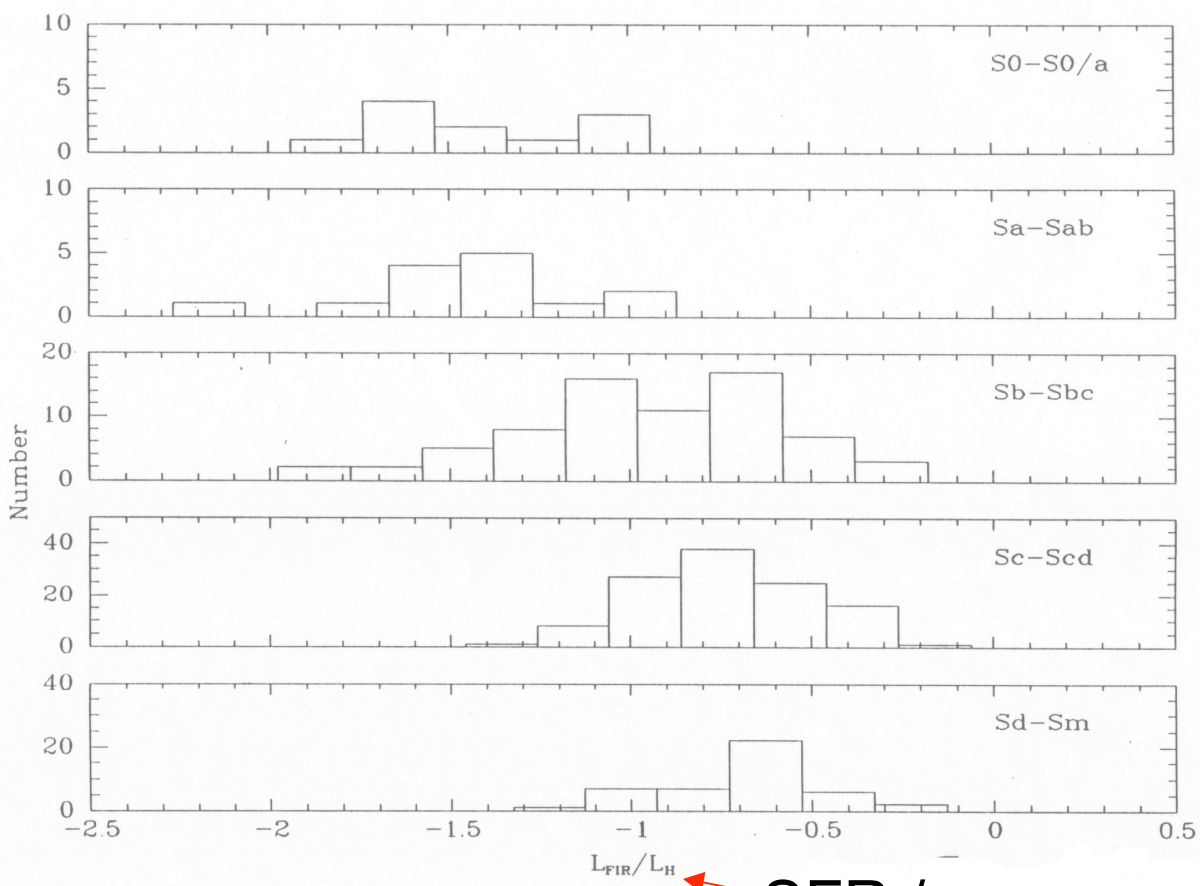

SFR / mass

Figure 4: *Distributions of 40- to 120-μm infrared luminosity for nearby galaxies, normalized to near-infrared H luminosity, as a function of Hubble type. Adapted from Devereux & Hameed (1997), with elliptical and irregular galaxies excluded.*

H-band (1.6 μm) = low mass stars = total mass of the system

Note that $SFR_{IR} > SFR_{UV\ or\ visual}$

- IR traces embedded SF in disk
- IR traces any nuclear SF that may be occuring
- IR also traces dust heated by the galactic radiation field, which has nothing to do with the present SFR
- The UV & visual trace only light from un-extinguished SF.

Schmidt Law

Consider that the SFR is proportional to the total amount of gas available,

$$\mathrm{SFR} \propto \rho_{\mathrm{gas}} \propto \frac{d\rho_{\mathrm{gas}}}{dt},$$

where ρ_{gas} is the gas density. Thus, the gas depletion is an exponential function of time,

$$\rho_{\mathrm{gas}} \propto \rho(0) e^{-t/\tau}$$

- This is the linear form of the Schmidt Law, & is used in most evolutionary models.

- A Starburst galaxy is a galaxy that would deplete its gas supply in a few dynamical times at its present SFR.

- Linear Schmidt Law shows SFR decreasing with time, which is contrary to what is observed.

Non-Linear Schmidt Law

A more generalized form of the law is

$$\mathrm{SFR} \propto \frac{d\rho_{\mathrm{gas}}}{dt} \propto \rho_{\mathrm{gas}}^{n}.$$

During interactions where gas may be compressed, $n > 1$, & star formation is enhanced.

In case of starburst activity, an estimation of n might be made by assuming that star formation is occuring at the timescale of free-fall collapse. Thus,

$$\mathrm{SFR} \propto \frac{\rho_{\mathrm{gas}}}{t_{\mathrm{freefall}}} \propto \frac{\rho}{\rho^{-0.5}} \propto \rho^{1.5}.$$

Star Formation in Spiral Disks

From $L_{H\alpha}$

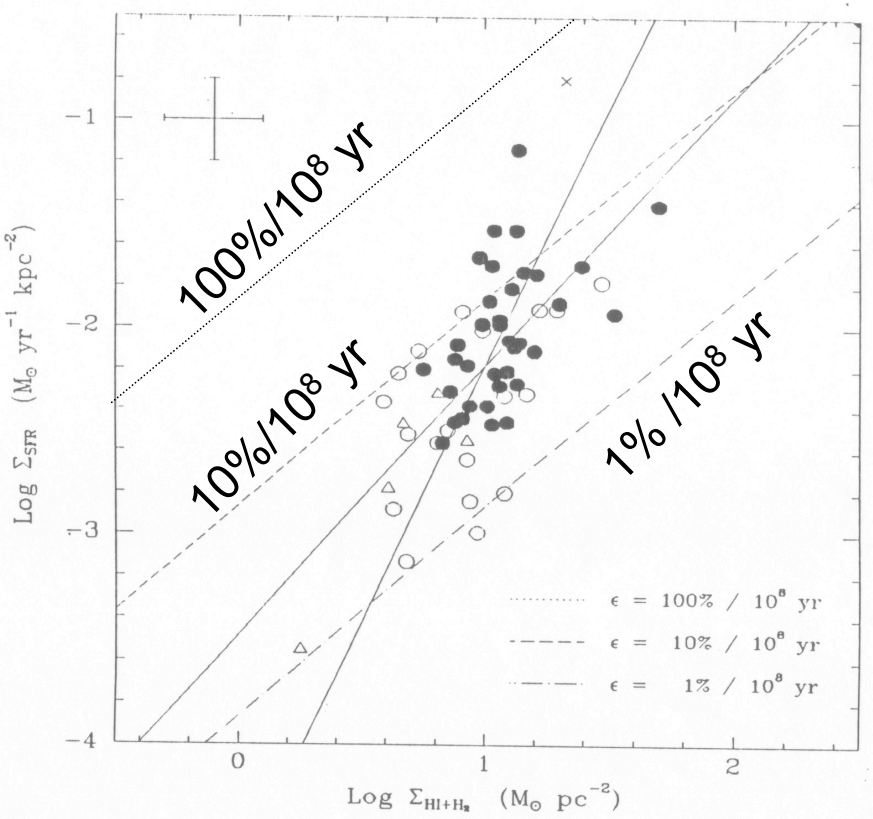

$$\Sigma_{\rm SFR} \propto \Sigma_{\rm gas}^{2.4}.$$

<4.8%> of gas every 10^8 yr

$\Delta t_{\rm disk} \approx t_{\rm Hubble}$

Gas depletion time-scale ≈ 2.1 Gyr

Figure 5: *Correlation between disk-averaged SFR per unit area and average gas surface density, for 61 normal disk galaxies. Symbols are coded by Hubble type: Sa–Sab (open triangles); Sb–Sbc (open circles); Sc–Sd (solid points); Irr (cross). The dashed and dotted lines show lines of constant global star formation efficiency. The error bars indicate the typical uncertainties for a given galaxy, including systematic errors.*

Star Formation Efficiencies

On the previous plot, lines of SF efficiencies per 10^8 yr are shown. The average efficiency for disk SF is 4.8% per every 10^8 years. The gas depletion time is thus,

$$10^8 \text{ yrs} \left(\frac{1}{0.048}\right) \sim 2.1 \text{ Gyr.}$$

I.e., uncomfortable short. The Sun makes 1 orbit around the galactic center every 2×10^8 yr, & thus would have only made,

$$\frac{2.1 \text{ Gyr}}{2.0 \times 10^8 \text{ yrs}} = 10 \text{ turns}$$

around the galactic center in this depletion time. Note, however, that recycling of gas through stellar mass loss & supernovae can increase this by a factor of 2 – 3.

Nuclear Star Formation

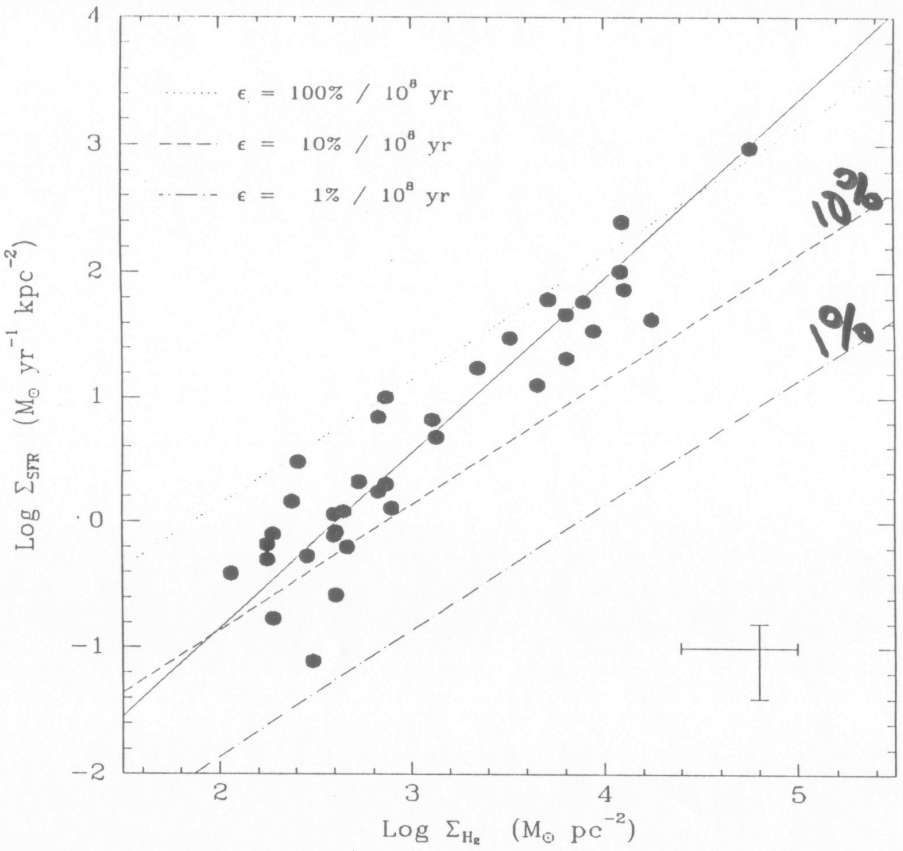

$$\Sigma_{\rm SFR} \propto \Sigma_{\rm gas}^{1.4},$$

<30%> of gas used
Every 10^8 yr

Depleted timescale
≈ 0.3 Gyr

Figure 7: *Correlation between disk-averaged SFR per unit area and average gas surface density, for 36 infrared-selected circumnuclear starbursts. See Figure 5 for a similar comparison for normal spiral disks. The dashed and dotted lines show lines of constant star formation conversion efficiency, with the same notation as in Figure 5. The error bars indicate the typical uncertainties for a given galaxy, including systematic errors.*

What if the SF efficiency is 100%?

Then,

$$\mathrm{SFR_{max}} = 100 \mathrm{M_\odot\ yr^{-1}} \left(\frac{M_{\mathrm{gas}}}{10^{10}\mathrm{M_\odot}}\right)\left(\frac{10^8\ \mathrm{yrs}}{\Delta t_{\mathrm{dyn}}}\right).$$

Considering:

1) 0.7% efficiency of conversion of mass → energy in stars
2) a fraction, ε, of the total stellar mass converted in 10^8 yr (ε = 0.05 for a Salpeter IMF),

The maximum luminosity produced by stars is,

$$L_{\mathrm{max}} = 0.07\epsilon\left(\frac{dM}{dt}\right)_{\mathrm{SFR}} c^2 = 7\times10^{11}\mathrm{L_\odot}\left(\frac{M_{\mathrm{gas}}}{10^{10}\mathrm{M_\odot}}\right)\left(\frac{\epsilon}{0.05}\right).$$

This is very near the maximum luminosity observed for IR starburst galaxies.

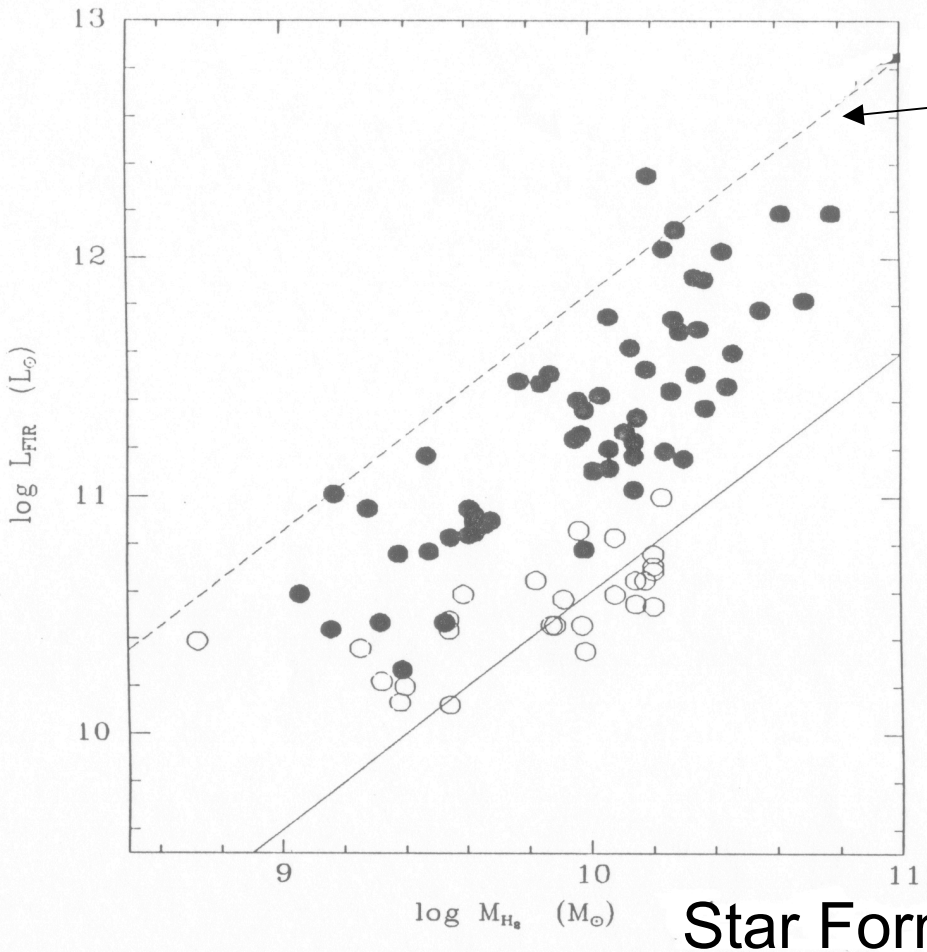

Figure 6: *Relationship between integrated far-infrared (FIR) luminosity and molecular gas mass for bright IR galaxies, from Tinney et al (1990; open circles) and a more luminous sample from Sanders et al (1991; solid points). The solid line shows the typical L/M ratio for galaxies similar to the Milky Way. The dashed line shows the approximate limiting luminosity for a galaxy forming stars with 100% efficiency on a dynamical timescale, as described in the text.*

Disk & Nuclear Star Formation

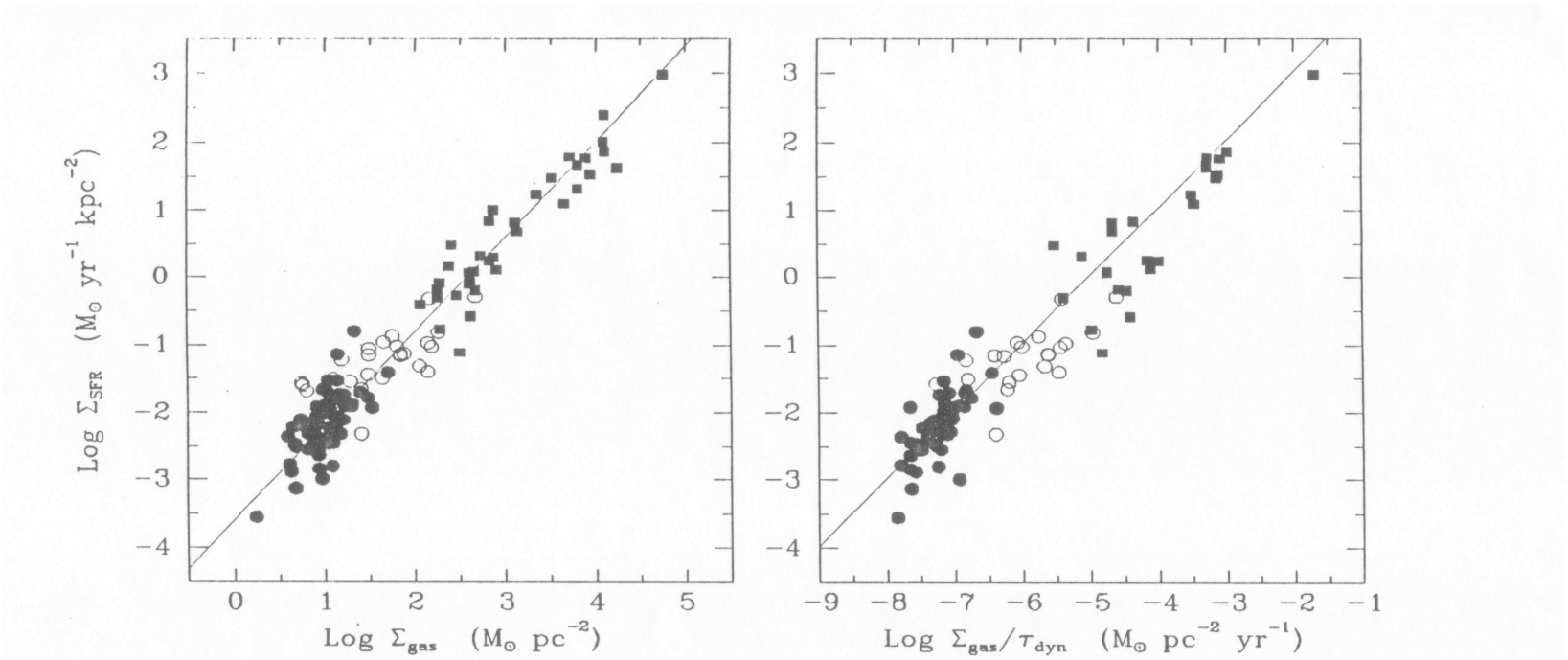

Figure 9: *(Left) The global Schmidt law in galaxies. Solid points denote the normal spirals in Figure 5, squares denote the circumnuclear starbursts in Figure 7. The open circles show the SFRs and gas densities of the central regions of the normal disks. (Right) The same SFR data, but plotted against the ratio of the gas density to the average orbital time in the disk. Both plots are adapted from Kennicutt (1998).*

$$\Sigma_{\rm SFR} = (2.5 \pm 0.7) \times 10^{-4} \left(\frac{\Sigma_{\rm gas}}{1 {\rm M}_\odot {\rm pc}^{-2}} \right)^{1.4 \pm 0.15} {\rm M}_\odot \ {\rm yr}^{-1} \ {\rm kpc}^{-2}.$$

Table 1: Star Formation in Disks and Nuclei of Galaxies

Property	Spiral Disks	Circumnuclear Regions
Radius	$1 - 30$ kpc	$0.2 - 2$ kpc
SFR	$0 - 20\ M_\odot\ yr^{-1}$	$0 - 1000\ M_\odot\ yr^{-1}$
Bolometric Luminosity	$10^6 - 10^{11}\ L_\odot$	$10^6 - 10^{13}\ L_\odot$
Gas Mass	$10^8 - 10^{11}\ M_\odot$	$10^6 - 10^{11}\ M_\odot$
Star Formation Timescale	$1 - 50$ Gyr	$0.1 - 1$ Gyr
Gas Density	$1 - 100\ M_\odot\ pc^{-2}$	$10^2 - 10^5\ M_\odot\ pc^{-2}$
Optical Depth (0.5 μm)	$0 - 2$	$1 - 1000$
SFR Density	$0 - 0.1\ M_\odot\ yr^{-1}\ kpc^{-2}$	$1 - 1000\ M_\odot\ yr^{-1}\ kpc^{-2}$
Dominant Mode	steady state	steady state + burst
Type Dependence?	strong	weak/none
Bar Dependence?	weak/none	strong
Spiral Structure Dependence?	weak/none	weak/none
Interactions Dependence?	moderate	strong
Cluster Dependence?	moderate/weak	?
Redshift Dependence?	strong	?

Stability due to Rotation

- How is the SFR correlated with gas surface density in spiral disks and nuclei?
- I.e., how does disk rotation effect the stability of gas in the disk

Consider a region of size l & mass surface density Σ_0 rotating with an angular speed ω at a distance r from the center of the galaxy.

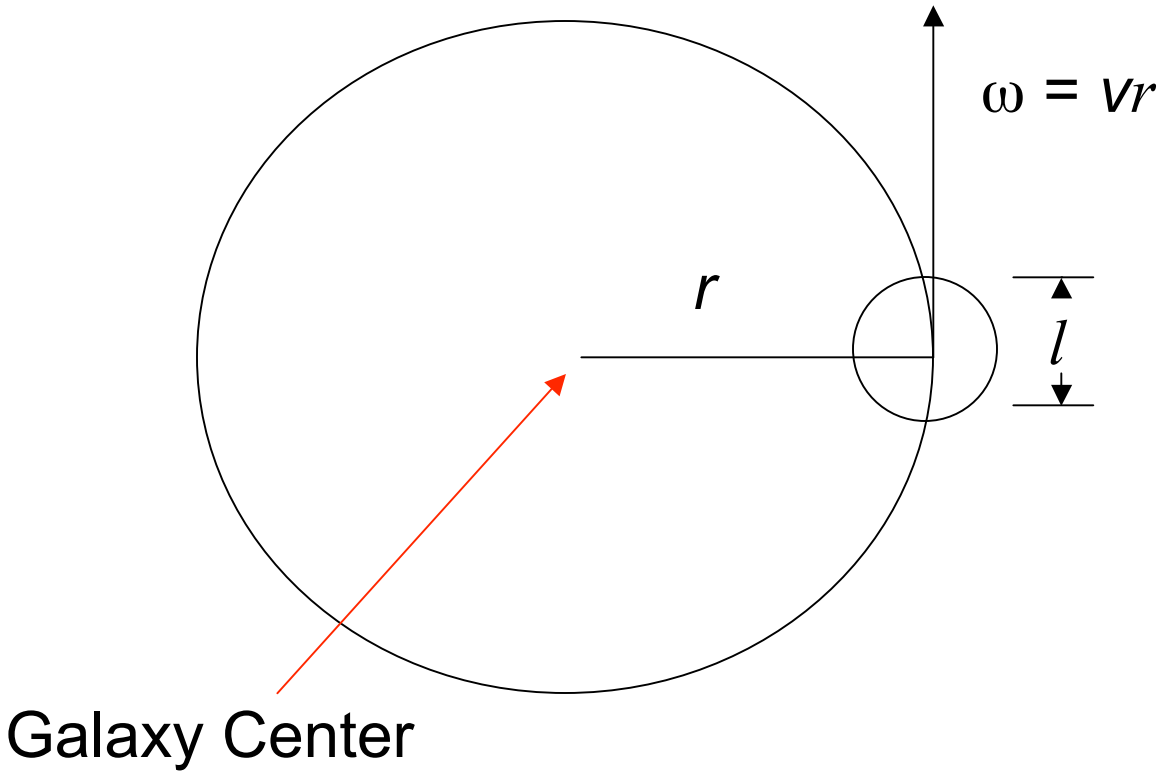

- A perturbation causes:

$$\text{an increase in mass surface density} = \epsilon\Sigma;$$

$$\text{a decrease in region size} = -\epsilon l;$$

$$\text{an increase in the gravitational force} = \frac{G\Sigma l^2}{(l-\epsilon l)^2} - \frac{G\Sigma l^2}{l^2} \sim 2\epsilon G\Sigma,$$

where mass = $\Sigma\, l^2$.

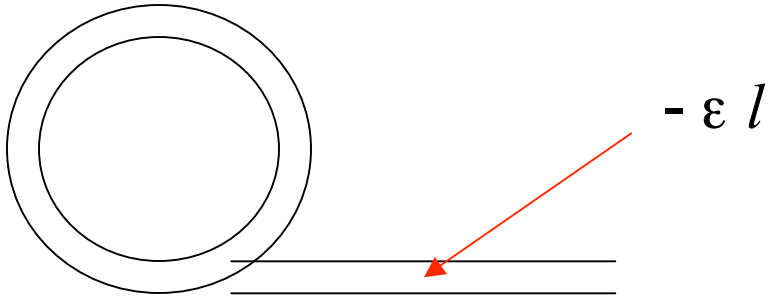

- The angular momentum,

$$J = vr = \omega r^2,$$

is conserved, thus J can be differentiated to get,

$$dJ = r^2 d\omega + \omega 2r dr = 0;$$

$$r^2 d\omega = -w2r dr;$$

$$\frac{d\omega}{\omega} = -2\frac{dr}{r} = \frac{2\epsilon l}{r},$$

where dr = - ε l.

- The centrifugal force increases by,

$$d(\omega^2 r) = \omega^2 dr + r2\omega d\omega;$$

$$= -\omega^2 \epsilon l + r2\omega \left(\frac{2\epsilon l}{r}\omega\right) = 3\epsilon l \omega^2.$$

- To have stability, the change in the gravitational force must balance the change in the centrifugal force,

$$2\epsilon G\Sigma = 3\epsilon l_{\rm crit}\omega^2,$$

And thus,

$$l_{\rm crit} = \frac{2G\Sigma}{3\omega^2}.$$

For collapse,

$$l < \frac{2G\Sigma}{3\omega^2}$$

Note that for gas in a circular orbit at r,

$$\omega^2 r = \frac{v^2}{r} = \frac{G\Sigma r^2}{r^2},$$

and thus,

$$r = \frac{G\Sigma}{\omega^2},$$

Thus, $r \sim l_{\text{crit}}$. I.e., galactic scales are stabilized by rotation, not local scales.

- What is the minimum velocity dispersion, σ, required to make the critical Jeans length ~ $l_{\rm crit}$?

$$t_{\rm freefall} = \left(\frac{l}{G\Sigma}\right)^{1/2} \quad \text{and} \quad t_{\rm cross} \sim \frac{l}{\sigma}.$$

So, equating them,

$$t_{\rm freefall} \sim t_{\rm cross};$$

$$\frac{l_{\rm Jeans}}{G\Sigma} \sim \frac{l_{\rm Jeans}^2}{\sigma^2};$$

$$l_{\rm Jeans} \sim \frac{\sigma^2}{G\Sigma}.$$

For stability,

$$l_{\rm Jeans} = l_{\rm crit};$$

$$\frac{\sigma^2}{G\Sigma} = \frac{G\Sigma}{\omega^2};$$

$$\sigma = \frac{G\Sigma}{\omega}.$$

For instability to occur,

$$\sigma > \frac{G\Sigma}{\omega}.$$

The actual equation in terms of the radial velocity, v_r, is

$$\sigma_r = \frac{3.36 G \Sigma}{\kappa},$$

where κ is the epicyclic frequency. The stability criterion is generally written in terms of the parameter Q such that,

$$Q = \frac{\text{observed } \sigma_r}{\text{critical } \sigma_r}.$$

If $Q > 1$, then there is stability.